Published in final edited form as:
Bioconjug Chem. 2007 ; 18(3): 903–911. doi:10.1021/bc060250q.

Peptidyl Molecular Imaging Contrast Agents Using a New Solid Phase Peptide Synthesis Approach

Byunghee Yoo and **Mark D. Pagel***
Case Center of Imaging Research and Department of Biomedical Engineering, Case Western Reserve University 10900 Euclid Avenue, Cleveland, OHIO 44106

Abstract

A versatile method is disclosed for solid phase peptide synthesis (SPPS) of molecular imaging contrast agents. A DO3A moiety was derivatized to introduce a CBZ-protected amino group and then coupled to a polymeric support. CBZ cleavage with Et_2AlCl/thioanisole was optimized for SPPS. Amino acids were then coupled to the aminoDOTA loaded resin using conventional step-wise Fmoc SPPS to create a product with DOTA coupled to the C-terminus of the peptide. In a second study, the DO3A moiety was coupled to a glycine-loaded polymeric support, and amino acids were then coupled to the amino-DOTA-peptide loaded resin using SPPS, to incorporate DOTA within the peptide sequence. The peptide-(Tm^{3+}-DOTA) amide showed a PARAmagnetic Chemical Exchange Saturation Transfer (PARACEST) effect, which demonstrated the utility of this contrast agent for molecular imaging. These results demonstrate the advantages of exploiting SPPS methodologies through the development of unique DOTA derivatives to create peptide-based molecular imaging contrast agents.

Keywords

DOTA; PARACEST; Caspase-3; MRI; Molecular Imaging

INTRODUCTION

Macrocyclic metal chelates using DOTA (1,4,7,10-tetraazacyclododecane-*N*,*N*’,*N*’’,*N*’’’-tetraacetic acid) are often administered to patients and animal models to create or enhance contrast in biomedical molecular imaging studies (1,2). More recently, metal-DOTA chelates have been conjugated to peptides to affect the in vivo pharmacokinetics of the metal-DOTA imaging agent over a wide range of spatial scales. For example, sub-cellular scales can be assessed by coupling DOTA to membrane-penetrating peptides (3,4), cellular scales are assessed with cell receptor-targeting peptides attached to DOTA (5), and tissue scales are investigated with DOTA-bound peptides that interact with extracellular matrices (6) and that have dramatically altered renal clearance rates (7). Numerous other applications have been reported, including peptide-DOTA probes for multimodality imaging studies (8–10).

*To whom correspondence should be addressed. Mark (Marty) Pagel, Ph.D., Case Center for Imaging Research, Assistant Professor of Biomedical Engineering, Case Western Reserve University, Tel.: +216 368 8519. Fax: 216 368 4969. E-mail: mpagel@case.edu.

[1]Abbreviation : Ac_2O, acetic anhydride; BaO, barium oxide; CCl_4, carbon tetrachloride; DCM, methylene chloride; DIEA, N,N-diisopropylethylamine; DMF, N,N-dimethylformamide; DO3A-tBu, 1,4,7,10-tetraazacyclododecane-*N*,*N*’,*N*’’-tri(tert-butylacetate); DOTA, 1,4,7,10-tetraazacyclododecane-*N*,*N*’,*N*’’,*N*’’’-tetraacetic acid; Et2AlCl, diethylaluminum chloride; Fmoc, fluorenylmethyloxycarbonyl; HBTU, 2-(1*H*-benzotriazole-1-yl)-1,1,3,3-tetramethyluronium hexafluorophosphate; HOBt, *N*-hydroxybenzotriazole; MeCN, acetonitrile; NMP, N-methylpyrrolidone; P_2O_5, phosphorous pentoxide; TEA, triethylamine.

To synthesize these peptidyl molecular imaging contrast agents, the carboxylates of DOTA have been conjugated to the amines of peptides, including the N-terminus of the backbone and the side chain of lysine (5,11–19). Other DOTA derivatives have been devised for conjugation to peptide amino groups, such as succinimide DOTA derivatives (20) and isothiocyanato DOTA derivatives (21). Unnatural amino acid derivatives have also been developed to couple DOTA to peptidyl amines, such as p-NH_2-phenylalanine (13) and diaminopropionic acid residues (15).

Standard solid phase peptide synthesis (SPPS) methods have been used to couple DOTA to the backbone N-terminus of peptides bound to a PEGA Rink amide resin (5,14–19). Similar SPPS methodologies can be used to couple DOTA to other side chain amines of resin-bound peptides (13,15). However, coupling DOTA only to N-terminus or side chain amines of peptides can limit synthesis methodologies and may compromise the utility of the peptidyl contrast agent for molecular imaging applications (22). To alleviate this limitation, we have developed an amine-derivatized DOTA (aminoDOTA) that can couple to the carboxylates of peptides (Scheme 1). We have linked the aminoDOTA to a resin **8a** for use in standard SPPS methodologies, in order to synthesize peptide- DOTA imaging agents with DOTA coupled to the C-terminus of the peptide (Scheme 2). We have also linked aminoDOTA to an amino acid residue on the resin **8b**, to demonstrate that this methodology can incorporate DOTA at any location within the peptide backbone (Scheme 1 and Scheme 2). Lanthanide chelates of the peptide-DOTA amide products were shown to affect magnetic resonance signals, thereby demonstrating that the peptide-bound DOTA moiety has practical utility for molecular imaging. This new approach greatly expands the opportunities to create peptide-based molecular imaging probes, and is completely compatible with standard SPPS methods for facile production of products with good yield and high purity.

EXPERIMENTAL PROCEDURES

General Methods

All the reactions were carried out under argon atmosphere. Dichloromethane (DCM) and carbon tetrachloride (CCl_4) were freshly distilled over phosphorous pentoxide (P_2O_5). Acetonitrile (ACN) was distilled over barium oxide (BaO). The peptide synthesis reagents Fluorenylmethyloxycarbonyl (Fmoc) protected amino acids, *N*-hydroxybenzotriazole (HOBt), 2-(1*H*-benzotriazole-1-yl)-1,1,3,3-tetramethyluronium hexafluorophosphate (HBTU), acetic anhydride (Ac_2O), piperidine, triethylamine (TEA), N,N-diisopropylethylamine (DIEA), N,N-dimethylformamide (DMF) and N-methylpyrrolidone (NMP) were purchased from Applied Biosystems Co. (Foster City, CA). The 1,4,7,10-tetraazacyclododecane-*N*,*N'*,*N''*-tri(tert-butylacetate) (DO3A-tBu) was purchased from Macrocyclics Co. (Dallas, TX), and other reagents were purchased from Sigma-Aldrich Corp. (St. Louis, MO) and Fisher Scientific International, Inc. (Hampton, NH). Peptides were synthesized using a Wang resin (Fluka, Buchs Switzerland) and followed Fmoc chemistry methods with HOBt and HBTU as coupling agents (23,24). The efficiencies of coupling DO3A-Fmoc **3** to resin **4b**, and coupling **6** to resin Fmoc-deprotected **5a** and **5b**, were checked with the Kaiser ninhydrin test (25–27). The starting resin had 1.0mmol/g of hydroxyl groups or amino groups and the scale of the peptide synthesis was calculated based on the substitution ratio of the resin. The loading efficiencies of the Fmoc-compounds and the amine content of the resin were quantitatively analyzed with UV/Vis/ Fluorescence spectroscopy using a Molecular Devices SpectraMax M2 spectrophotometer. IR spectroscopy was used to analyze the functional groups on the resin using an ABB BOMEM MB-104 spectrophotometer operating from 600 to 4000cm−1. To analyze the peptides and the peptide-DOTA amide final product, HPLC was used with a Grace Vydac OD-300 C-18 reverse phase analytical column and a PerkinElmer Series 200 HPLC pump and UV detector operating at 222 nm. The lanthanide complexation reaction between peptide- DOTA amide and $TmCl_3$

was evaluated with an Arsenazo III solution color test (28,29). ^{1}H and ^{13}C spectra were measured with a Varian Gemini 300MHz NMR spectrometer and Varian Inova 600MHz NMR spectrometer using $CDCl_3$ and DMSO-d_6 as solvents depending on solubility. PARAmagnetic Chemical Exchange Saturation Transfer (PARACEST) spectra were measured in a solution of 5% D_2O in water (30,31) using a Varian Inova 600 MHz NMR spectrometer. A series of 1D NMR spectra of the water signal were acquired with a selective saturation in 1ppm increments between 100 ppm and −100 ppm, and selective saturation was performed with a continuous wave pulse applied for 4 seconds at 31 μT. Analytical thin layer chromatography was performed on Merck silica gel 60 F254 plates. Compounds were visualized using a UV lamp operating at 254 nm, an iodine chamber and ninhydrin solution. High resolution mass spectral analyses were performed with Bruker Daltonics Esquire HCT mass spectrometer and a Bruker BIFLEX III MALDI-TOF mass spectrometer, using 3,5-dimethoxy-4-hydroxycinnamic acid as a matrix compound. Molecular modeling was accomplished using InsightII with the Discover-3 (Molecular Simulations Inc.).

Synthesis & Analysis

Synthesis of 4,7,10-tri(t-butylacetate)-1-fluorenylmethoxycarbonyl-1,4,7,10-tetraazacyclododecane (Fmoc-DO3A-tBu) 2 (32)—To a solution of **1** (2.57 g, 5mmol) in 10 mL of acetonitrile, activated zinc dust was added in small portions until the reaction mixture attained neutral pH. A solution of Fmoc-Cl (1.35 g, 5 mmol, 1 eq.) in 5 mL of ACN and zinc dust (325 mg, 5 mmol, 1 eq.) was added to the reaction mixture in one portion and the reaction mixture was stirred at room temperature for 20 min. The progress of the reaction was monitored by TLC ($CHCl_3$/MeOH=1/1, Rf=0.75). The reaction mixture was filtered and dried in vacuo, yielding 3.32 g of white solid (yield 90%): ^{1}H NMR (600MHz, DMSO-d_6) δ 1.47(s, 27H), 2.50(s, 8H), 2.71(t, 4H), 2.79(t, 4H), 3.39(s, 6H), 5.15(t, 1H), 6.29(d, 2H), 7.42 (t, 2H), 7.47(t, 2H), 7.63(d,2H), 7.84(d, 2H), ^{13}C (125MHz, DMSO-d_6) δ 170.61, 153.83, 135.59, 135.36, 129.47, 127.23, 123.88, 121.36, 119.99, 81.22, 65.88, 55.14, 53.53, 50.48, 48.44, 47.10, 27.75, MALDI-Mass *m/z* (calc. 736.94): 737.96 $[M+H]^+$.

Synthesis of 4,7,10-tri(carboxymethyl)-1-fluorenylmethoxycarbonyl-1,4,7,10-tetraazacyclododecane (Fmoc-DO3A) 3—A total of 2.94 g (4 mmol) of **2** was dissolved in 5 mL of 75% TFA in DCM and treated for 40 min. The reaction was traced by TLC (chloroform/methanol=1.1, Rf=0.22). The solution was dried under reduced pressure. The remaining solid was re-dissolved in DCM and precipitated with diethyl ether. The precipitated solid was filtered and dried in vacuo, yielding 1.70 g (3.0 mmol, yield 75%): ^{1}H NMR (600MHz, DMSO-d_6) δ 3.05(s, 4H), 3.20(s, 4H), 3.45(t, 4H), 3.62(t, 4H), 3.60(s, 6H), 4.25(t, 1H), 4.55(d, 2H), 7.35(t, 2H), 7.42(t, 2H), 7.65(d,2H), 7.94(d, 2H), ^{13}C (125MHz, DMSO-d_6) δ 174.21, 155.44, 143.85, 140.63, 127.08, 125.07, 120.01, 67.24, 54.30, 51.88, 50.65, 48.68, 45.79, MALDI-Mass *m/z* (calc. 568.62): 569.64 $[M+H]^+$.

Coupling of Fmoc-DO3A on the resin 5a, 5b—To prepare 5a, 1.0 g of Wang resin **4a** (substitution level = 1 mmol/g) was used after complete drying. The compound **3** (1.14 g, 2 mmol), HBTU (2.5 g, 6.6 mmol, 3.3 eq.) and HOBt (1.0 g, 6.6 mmol, 3.3 eq.) were dissolved in 30 mL of NMP for 40 min to activate carboxylates, and the solution was added to the peptide reaction vessel containing the resin. TEA (1.82 mL, 13 eq.) was added and the reaction was continued for 12 h. After filtration, the resin was dispersed in a solution of tert-butyl alcohol (t-BuOH, 1.48 g, 20 mmol, 20 eq.) in 20 mL of NMP and the reaction was continued for 1 h. The resin was washed and dried in vacuo. To prepare **5b**, 1.3 g of **4b** (substitution level = 0.78 mmol/g) was treated with **3** following the same synthetic method as **4a**. During the reaction, a small amount of resin was sampled for uncoupled amines using the Kaiser test.

Loading Efficiency (Fmoc titration)—The Fmoc concentration on the resin was measured according to a previously reported method (33). Fmoc amino acyl resins (4~8 mg) were shaken or stirred in piperidine- DMF (3:7) (0.5 mL) for 30 min, after which MeOH (6.5 mL) was added and the resin was allowed to settle. The resultant fulvene-piperidine adduct had UV absorption maxima at 267 nm ($\varepsilon = 17{,}500\ M^{-1}cm^{-1}$), 290 nm ($\varepsilon = 5800\ M^{-1}cm^{-1}$), and 301 nm ($\varepsilon = 7800\ M^{-1}cm^{-1}$). For reference, a piperidine-DMF-MeOH solution (0.3:0.7:39) was prepared. Spectrophotometric analysis was carried out at 301 nm, with comparison to a free Fmoc amino acid (Fmoc-Ala) of known concentration treated under identical conditions. The measured Fmoc concentrations were determined to be 0.45 (± 0.05) mmol per gram of resin (calc. 0.64 mmol/g) for **5a** and 0.47 (± 0.05) mmol per gram of resin (calc. 0.54 mmol/g) for **5b**, based on 3 repetitions to synthesize each product.

Methyl N-(Benzyloxycarbonyl)-α-bromoglycinate 6—Phosphorous tribromide (8.2 g, 30 mmol, 3 eq.) was added to a suspension of methyl N-(Benzyloycarbonyl)-α-methoxyglycinate (2.51 g, 10 mmol) in carbon tetrachloride (100 mL) under an argon atmosphere. The reaction mixture was stirred at room temperature for 7 days. The reaction solution was then concentrated in vacuo and triturated with dry n-hexane (100 mL) for 24 hrs. The reaction mixture was then filtered, yielding a white solid (75% to quantitative yield measured by weight): ^{1}H NMR (300MHz, $CDCl_3$) δ 3.80(s, 3H), 5.22(s, 2H), 6.20 and 6.45 (split, 1H), 7.55(s,5H); ^{13}C (125MHz, DMSO-d_6) δ 170.71, 156.07, 137.37, 129.03, 128.57, 128.53, 73.78, 66.25; MS-ESI *m/z* (calc. 302.99): 304.07 $[M+H]^+$

Coupling of 6 on the resin 7a, 7b—Each of **5a** (2.22 g, substitution level =0.45 mmol/g) and **5b** (2.13 g, substitution level =0.47 mmol/g) were treated with 20% piperidine for 30 min and sequentially washed with NMP, DCM, acetone, and acetonitrile. The Kaiser test was used to measure the content of free secondary amines after Fmoc deprotection. The resin was transferred to a flask with **6** (0.6 g, 2 mmol, 4.3 eq.) and K_2CO_3 (1.66 g, 12 mmol, 25.5 eq.) in dry acetonitrile (100 mL). The solution was stirred and heated to 70 °C for 6 h in anhydrous conditions. After the solution was filtered, the resin was sequentially washed with 50% MeOH in water, MeOH, and DCM, and then dried in vacuo. The Kaiser test was used to monitor the coupling of **6** to **7b** by measuring the concentration of remaining free amines.

Cleavage of CBZ group from the resin 8a, 8b—In each of 3 flasks, 0.20 g (0.1mmol) of **7a** was dispersed and swelled in DCM (5 mL) for 1 h and cooled to −78 °C. Et_2AlCl (34) was transferred into each flask with an air-tight syringe in 1, 2 and 5 eq. and the mixture was stirred for 15 min. Aliquots of 2, 4, and 10 eq. of thioanisole (the molar ratio of Et_2AlCl:thioanisole was fixed at 1:2) was added to each flask and portions of the resin were extracted after 5, 15, 30 and 60 min of cleavage reaction time. The sampled resin was immediately washed with DCM and titrated with picric acid according to a previously reported method (35). To account for tertiary amines on the cyclen ring, a CBZ protected resin was treated and compared as a reference. CBZ cleavage was performed with conditions of 1 eq. of 33% Et_2AlCl in thioanisole for 20 min at 7−78 °C. The average amine content was 0.31 (±0.05) mmol/g for **8a** and 0.33 (±0.05) mmol/g for **8b**, based on 3 repetitions to synthesize each product.

Peptide synthesis 9a, 9b—A total of 1.63 g (0.5 mmole) of **8a** was used to synthesize **9a** using standard SPPS methods. Fmoc-Asp(O^{t}Bu)-OH (0.2 g, 0.5 mmol), Fmoc-Val-OH (0.17 g, 0.5 mmol) and Fmoc-Glu(O^{t}Bu)-OH (0.23 g, 0.5 mmol) were used as building amino acids and HBTU (0.19 g, 0.5 mmol) and HOBt (73 mg, 0.5 mmol) were used as coupling agents. Freshly distilled TEA (140 μL, 1 mmol) was used as a base in 70 mL of NMP. A solution of 20% piperidine in NMP was used to cleave the Fmoc groups on the resin, after which 1 equivalent of an amino acid was reacted with the resin-bound peptide-DOTA amine.

This coupling was repeated with a second reaction that was not preceded with Fmoc deprotection, in order to follow a double-coupling SPPS strategy, which yielded 1.94 g of **9a** (calc. 1.97 g, yield 93%). Using the same procedure, 0.42 g (0.14 mmole) of **8b** was treated to synthesize 0.50 g of **9b** (calc. 0.52 g, yield 90%).

Peptide cleavage from the resin and characterization of 10a and 10b—After the peptide synthesis, the Fmoc group of **9a** (0.55 g, 0.2 mmole) was removed from the resin and **10a** was cleaved from the resin with a 95% TFA / 2.5% water / 2.5% thioanisole cocktail for 40 min (36–38). After removing solvents, the product was washed with diethylether and dried in vacuo. The final product was purified with an amberlite column, yielding 150 mg (0.17 mmol, yield 85%). Following the same procedure, 0.29 g of **9b** (0.1mmole) was used to obtain 87 mg of **10b** (92 μmole, yield 92%). In both cases, the amberlite column was used to remove impurities and residue from the cleavage cocktail, and was not intended to purify isomeric forms of 10a or 10b. The obtained products **10a** and **10b** were characterized by MALDI-MASS (**10a** *m/z* (calc. 891.88): 892.89 $[M+H]^+$, 914.89 $[M+Na]^+$; **10b** *m/z* (calc. 948.93): 949.94 $[M+H]^+$, 971.95 $[M+Na]^+$) and HPLC (Column : Symmetry C-18 3.5um, 4.6 × 75mm, Detector : 222 nm, Flow rate : 0.5 mL/min, Eluent : 0.1% TFA in water / acetonitrile, gradient from 100% / 0% to 90% / 10% for 5 min, 90%/10% for 25min; retention time = 6.1 min for **10a** and **10b**).

Complexation of Tm^{3+} with 11a, 11b—The obtained **10a** (100 mg, 0.11 mmol) was dissolved in water (3 mL) at pH 6.5 and 40 °C, and $TmCl_3$ (27 mg, 0.1 mmol) in water (0.5 mL) was added drop by drop for 1 hr and adjusted to pH 7.5 with 0.5N NaOH. The solution was stirred for 18 hrs at 40 °C and adjusted to pH 7.5 when the pH dropped below 5. The complete complexation was evaluated with an Arsenazo III color test (29). When the test showed negative results for free lanthanide ions, the reaction mixture was cooled to room temperature. The pH was adjusted to 9 and the residual lanthanide-hydroxide white precipitate was removed by filtration. The solution was freeze dried, yielding product **11a** (MALDI-Mass *m/z* (calc. 1060.81): 1061.83 $[M+H]^+$, 1083.85 $[M+Na]^+$). **10b** was treated with a similar procedure to obtain the final product **11b** (MALDI-Mass *m/z* (calc. 1117.86): 1118.87 $[M+H]^+$, 1140.92 $[M+Na]^+$).

RESULTS AND DISCUSSION

Scheme 1 demonstrates the synthesis strategies that were employed to create a DOTA-loaded resin for SPPS. Compound **2** was prepared by coupling **1** and Fmoc-Cl with activated Zn dust (32). Consequently, **2** was treated with 75% TFA in DCM for 40 min to remove ^{t}Bu esters. The deprotected product was a complex of **3** and TFA salt, as indicated by the NMR chemical shifts of the cyclen ring that were shifted to 3.05–3.62 ppm, relative to the NMR chemical shifts of 2.50–2.79 ppm of the cyclen ring of TFA-free **2**.

Compound **3** was coupled to a Wang resin **4a** (sub.lev. = 1.0 mmol/g) and a glycine-preloaded Wang resin **4b** (sub. lev. = 0.78 mmol/g) to create **5a** and **5b**, respectively. Compound **4b** was prepared to demonstrate the feasibility of incorporating DOTA within a peptide sequence. Compounds **5a** and **5b** showed 70% loading and 83% loading, respectively, as measured by quantitatively titrating the Fmoc group with a UV spectrometer operating at 301 nm wavelength. The lower loading of **5a** relative to **5b** is presumably caused by the closer proximity required by the hydrophilic **3** and the relatively hydrophobic surface of **5a**, in order to couple **3** to the short linker of **5a**. Adding an amino acid to the Wang resin lengthened the linker in **5b** and led to an improved loading efficiency, and comparable or improved results are anticipated if the Wang resin is pre-loaded with a longer peptide that would have even less potential for potentially adverse DOTA-resin interactions.

At the end of the coupling reaction to create **5a** and **5b**, an excess amount of *t*-BuOH was added to convert the remaining active carboxylates to *t*-Bu esters, and finally acetic anhydride was used to cap remaining functional active sites on the Wang resin (39,40). No active sites remained after this esterification and capping, because analysis of **10a** and **10b** showed no evidence of synthesized peptide without DOTA, or DOTA coupled to more than one peptide, which would be expected from any active sites that remain at this stage.

For clarity, Scheme 1 only shows coupling to the Wang resin at position 1 and Fmoc protection at position 4 (or 10) of the cyclen ring, and yet the Fmoc protection may also occur at position 7. This difference is inconsequential for **5a**, because the resin is eventually cleaved from the DOTA to create **10a**. This difference may be significant for **5b**, as the two peptidyl ligands of **10b** may have a 1,4 or 1,7 configuration. For comparison, studies of 1,4-DO2A vs 1,7-DO2A have demonstrated that the 1,4 isomer makes a more stable complex with Manganese (41). Studies of RRSS and RSRS tetra(carboxyethyl) DOTA derivatives indicated different ratios of the 'major' square antiprismatic geometric isomer (M) vs the 'minor' twisted square-antiprismatic geometric isomer (m), although no significant differences in hydration states were observed from these particular isomers (42). Yet the stabilities, hydration states and water exchange rates of DOTA derivatives are known to be affected by different m/M geometric ratios (43,44). Therefore, more detailed investigations of the effects of 1,4 and 1,7 isomers on stabilities and water exchange rates of DOTA derivatives are warranted, and the SPPS methodology described herein may provide the versatility for synthesizing isomers for these investigations.

The α-bromo glycine template **6** was produced as racemates at approximately a 1 to 1 ratio, which was indicated by the NMR doublet on 5.20 and 5.46 ppm. The diastereomers of consequent steps were also determined to be the same ratio as **6**. The presence of diastereomers within a peptide may raise concerns because peptide conformations critically depend on the stereochemistry of each amino acid. However, this strategy to conjugate DOTA to peptide carboxylates is intended to label a peptide with an imaging contrast agent, and is not designed so that the DOTA directly participates in the conformation or biological function of the peptide. Therefore, racemization of **6** is acceptable for molecular imaging applications that simply require DOTA-labeling of peptides. The use of brominated amino acid templates provides additional flexibility for creating peptide-DOTA imaging contrast agents, although other brominated amino acids besides bromoglycine were not investigated in this particular study.

After removal of the Fmoc group of **5a** and **5b** with 20% piperidine in NMP, **5a** and **5b** were coupled with α-brominated CBZ-Gly-OMe (45) **6** to obtain **7a** and **7b**, respectively. A comparison of results from the Fmoc titration and a Kaiser test of Fmoc-deprotected **5a** and **5b** indicated complete removal of the Fmoc groups. Similarly, a Kaiser test of **7a** and **7b** indicated that loading **6** onto the resin was performed with quantitative yield.

The CBZ group is commonly used to orthogonally protect amine groups in organic syntheses. Cleavage of CBZ groups is typically performed with H_2/Pd-C or 1,4-cyclohexadiene/Pd-C in EtOH (46). However, these cleavage conditions are not compatible with SPPS using polymeric supports, which lead to difficult problems with separation and purification. In this study, selective CBZ cleavage conditions were tested for SPPS. $BF_3{\cdot}Et_2O$/dimethylthioether (47–49), trimethylsilyl iodide (50,51) and Et_2AlCl/thioanisole (34) conditions were investigated during initial trials. From the results of tracing the reactions for **7a** and **7b** with the Kaiser test, the strong Lewis acids $BF_3{\cdot}Et_2O$/dimethylthioether and trimethylsilyl iodide were found to rapidly cleave the Wang linker on the resin, and therefore failed to selectively cleave the CBZ group. Fortunately, the CBZ group was found to be selectively cleaved with Et_2AlCl/thioanisole by reducing the temperature to −78 °C and by carefully controlling the reaction time and molar ratio of Et_2AlCl/thioanisole to optimize reaction conditions (Figure 1). The

reaction rates were assessed by measuring the amine contents of ~25 mg of resin after the start of the reaction, by using a picric acid titration and a UV/Vis spectrometer operating at 358 nm (35). These results were compared to the measured Fmoc concentrations of **5a** and **5b**. To eliminate the effect of tertiary amines in the cyclen ring, the results of picric acid titration of **7a** and **7b** that were not subjected to Et_2AlCl/thioanisole was subtracted from the measurements of the cleavage reaction. Optimized conditions were determined to consist of a reaction time of 15 min at −78°C, 1 eq. of Et_2AlCl and 2 eq. of thioanisole relative to the CBZ concentration on the resin. Under these conditions, cleavage of the benzyl ether group of the Wang linker or incomplete CBZ cleavage limited the overall yield of **8a** and **8b** to 70%. For the purposes of this particular study, a 70% yield was acceptable for subsequent steps. Although cross-linking between DOTA carboxylates and amines may also account for reduced yield after CBZ cleavage, MALDI-MS analyses of **10a** and **10b** showed no evidence for cross-linking, which is presumably due to the sparse population of DOTA within the Wang resin.

Additional temperature- and time-dependent studies to improve this deprotection step are under investigation in our laboratory, as CBZ deprotection during SPPS has great potential for orthogonal synthetic strategies. The expected transition state is shown in Figure 2. Previous reports have shown that Et_2AlCl can bridge two carbonyl groups in a 1,3-position to form a stable 6-membered ring, which leads to bond cleavage adjacent to either carbonyl group (52–53). However, Et_2AlCl would form an unstable 7-membered ring by bridging the two carbonyl groups of CBZ-Gly-OMe, and this bridge would be further destabilized by the additional planar constraints of the amide and ester groups, so that Et_2AlCl is more likely to form a strong interaction with just one carbonyl group. This hypothesis is confirmed by the absence of cleavage of the methyl ester group as shown in the mass spectrum of **10a** and **10b**, which also shows that the interaction of Et_2AlCl only occurs with the ester of the CBZ group.

As shown in Scheme 2, conventional Fmoc SPPS methods were then employed to perform step-wise coupling of amino acids to the aminoDOTA Wang resin (33). An Asp-Glu-Val-Asp (DEVD) peptide sequence was chosen for this demonstration, because this peptide sequence is preferentially cleaved by the caspase-3 enzyme that is a focus of our molecular imaging research (55). To enhance the coupling efficiency, two sequential applications (i.e., double coupling) of 4 equivalents of each amino acid was applied to the SPPS after initial Fmoc deprotection. The total yield of step-wise SPPS of the four amino acids to amino-DOTA was 90% and 93% for the synthesis of **10a** and **10b**, respectively, as determined by weighing. Therefore the coupling efficiency for coupling the first amino acid to amino-DOTA is no lower than 93%. This high coupling efficiency indicates that the CBZ-protected amine is sufficiently exposed after deprotection, even in the presence of the bulky DOTA moiety.

The SPPS products **10a** and **10b** were cleaved from the resin **9a** and **9b**. HPLC analyses of **10a** and **10b** showed a single peak, indicating that the peptide was successfully synthesized without additions or deletions of amino acids. HPLC analyses showed no evidence for separating stereoisomers of **10a** or **10b**, or different relative ligand positions around the cyclen ring of **10b**.

These SPPS products **10a** and **10b** were used to chelate thulium using standard conjugation methods and an Arsenazo III color test (29) to create **11a** and **11b**. The weight of the reactants (including salt) and product indicated that the chelation was quantitative. Although the final product was not desalted to approximate isotonic conditions during subsequent analyses, the presence of salts did not affect the determination of yield. In addition, mass spectrometry did not detect the presence of **10a** or **10b**, further indicating that the complexation was quantitative. However, low amounts of unchelated **10a** and **10b** may still exist within the final product. Chelation of the lanthanide ion required lower temperatures and shorter reaction times relative to lanthanide chelations of DOTA-amide derivatives prepared in our laboratory. This facile

chelation is attributed to the presence of 3 carboxylates and 1 carbonyl in **10a** and 2 carboxylates and 2 carbonyls in **10b** that participate in metal chelation, relative to metal chelation with amide carbonyl groups in DOTA-amide derivatives. These results are similar to detailed chelation studies of other DOTA derivatives that indicate the advantage of employing carboxylates for metal-binding, (56,57) and may indicate an improved stability and reduced toxicity of **11a** and **11b** relative to DOTA-amide formulations. Deprotection of the methyl ester of 11a or 11b would improve chelation. This deprotection was not performed in this study, because the methyl ester group provides unique functionality for further derivitization of the peptide's C-terminus.

To demonstrate the application of the final product for molecular imaging, **11a** and **11b** were detected through the effect of PARAmagnetic Chemical Exchange Transfer (PARACEST) (30,31). The PARACEST effect is created by saturating a unique NMR chemical shift corresponding to an amide hydrogen (or more generally, a hydrogen of a functional group that that exchanges with water at a rate of approximately 100–5000 sec^{-1}), and the effect is detected by observing a decrease in the water signal caused by transferring the saturation through chemical exchange. This novel mechanism for detecting imaging contrast agents has many advantages for biomedical applications that use magnetic resonance imaging. PARACEST exploits the close proximity between the amide group and the lanthanide ion to create a very unique NMR chemical shift for the amide group of the imaging agent, which facilitates selective saturation of this chemical shift. The synthesis strategy presented in this report is specifically designed to place amide groups in close proximity to the lanthanide ion.

Selective radio frequency irradiation at −51 ppm created a 7.8% PARACEST effect from 25 mM of **11a** (Figure 3). This PARACEST effect of **11a** occurs at the same chemical shift frequency and at a similar signal strength reported for a similar compound, DOTAMGly-Tm^{3+} (58). In addition, the PARACEST effect of **11a** shows good sensitivity at physiological pH and temperature, indicating that this contrast agent can be used for in vivo molecular imaging (Figure 4).

A similar PARACEST effect of 7.3% was observed from 12 mM of **11b**. The PARACEST effects from the two amide hydrogens (Hb and Hc in Figure 5) both occurred at −51 ppm and were not distinguishable. To investigate the basis for this similarity, molecular modeling of the DOTA core of **11b** was performed with carboxylates constrained to conjugate the Tm^{3+} ion. These results revealed that Hb is positioned 4.1–4.3 angstroms from Tm^{3+}, and Hc is positioned 4.9–5.1 angstroms from Tm^{3+}. Although a more detailed analysis of Tm^{3+} molecular orbitals is required for an accurate analysis of NMR chemical shifts, the very similar proximities of Hb and Hc to the lanthanide ion is sufficient to justify indistinguishable PARACEST effects that are measured in relatively coarse 1 ppm increments. The PARACEST effect is proportional to the number of water-exchangeable hydrogens that have the same NMR chemical shift. **11b** showed a PARACEST effect that was twice as strong as **11a** (on a per molar basis), demonstrating that multiple peptidyl ligands can improve the detection sensitivity of PARACEST imaging contrast agents.

This synthesis methodology may also be applied to couple peptides to other metal chelators that are used for molecular imaging. For example, diethylenetriaminetetraacetic acid (DTTA) may be used in place of **1** to couple a peptide to diethylenetriaminepentaacetic acid (DTPA) (1,59). To couple more than 2 peptides to a molecular imaging contrast agent, 1,4,7,10-tetraazacyclododecaneacetic acid (DO1A) may be used in place of **1** to couple 3 peptides to DOTA following the scheme to synthesize **10a**, or to couple 4 peptides to DOTA following the scheme to synthesize **10b**. Similarly, diethylenetriamineacetic acid (DT1A) may be used in place of **1** to couple 4 or 5 peptides to DTPA.

Larger derivatives of DOTA and DTPA, such as hexaazacyclohexadecane-N,N',N'',N''',N'''',N'''''-hexaacetic acid (HEHA) (60) and triethylenetetraaminehexaacetic acid (TTHA) (61), provide opportunities to couple additional peptides to a single molecular imaging agent. If the chemical shifts of all amides within multiple peptide-chelator linkages have the same MR chemical shift, then exploiting this SPPS method to link multiple peptides to a single chelator may increase the strength of the PARACEST effect and improve the detection of these molecular imaging contrast agents.

This synthesis methodology may address other important applications in molecular imaging. The employment of standard SPPS techniques provides a convenient and robust method for synthesizing libraries of molecular imaging contrast agents, which may be useful for high throughput screening to identify molecular imaging contrast agents with optimal properties. Because DOTA macrocyclic rings can strongly chelate a variety of ions, the peptide-DOTA product can be used to develop molecular imaging contrast agents for relaxivity-based MRI using Gd^{3+} or Dy^{3+} (1,62), or for nuclear imaging using ^{64}Cu (63) or ^{111}In (64), in addition to PARACEST MRI as demonstrated in this report. Therefore, this synthesis strategy represents a platform technology for molecular imaging.

CONCLUSION

To summarize, a new SPPS approach has been developed to couple DOTA to the C-terminus of a peptide, and to incorporate DOTA within the peptide sequence, in order to synthesize peptidyl contrast agents for molecular imaging. The selective cleavage of CBZ protecting groups in SPPS was investigated and optimized for the DOTA-loaded resin. The CBZ deprotection step and the step to load DOTA onto the resin were accomplished with acceptable yields for SPPS. Although R,S stereoisomers and 1,4 & 1,7 ligand isomers didn't affect subsequent analyses in this report, the effect of isomeric forms on chelation stability, hydration and water exchange rates is warranted, and development of isomeric forms for studies of isomers may be facilitated by this new SPPS strategy. Peptide-DOTA products were used to chelate thulium to create PARACEST imaging contrast agents that demonstrated good detection sensitivities at physiological conditions. This synthesis strategy provides great flexibility for coupling one or more peptides to DOTA to create peptide-DOTA imaging contrast agents for many molecular imaging applications.

ACKNOWLEDGMENT

This work was supported by the U.S. Army Medical Research and Materiel Command under #W81XWH-04-1-0731. This work was also supported by the Northeastern Ohio Animal Imaging Resource Center, an NIH funded program #R24CA110943, as part of the Case Center for Imaging Research.

LITERATURE CITED

1. Caravan P, Ellison JJ, McMurray TJ, Lauffer RB. Gadolinium(III) Chelates as MRI Contrast Agents: Structure, Dynamics, and Applications. Chem. Rev 1999;99:2293–2352. [PubMed: 11749483]
2. Anderson CJ, Welch MJ. Radiometal-labeled agents (non-technetium) for diagnostic imaging. Chem Rev 1999;99:2219–2234. [PubMed: 11749480]
3. Allen MJ, Meade TJ. Synthesis and visualization of a membrane-permeable MRI contrast agent. J. Biol. Inorg. Chem 2003;8:746–750. [PubMed: 14505078]
4. Prantner AM, Sharma V, Garbow JR, Piwnica-Worms D. Synthesis and characterization of a Gd-DOTA-D-permeation peptide for magnetic resonance relaxation enhancement of intracellular targets. Molecular Imaging 2003;2:333–341. [PubMed: 14717332]
5. De Leon-Rodriquez LM, Ortiz A, Weiner AL, Zhang S, Kovacs Z, Kodadek T, Sherry AD. Magnetic resonance imaging detects a specific peptide-protein binding event. J. Am. Chem. Soc 2002;124:3514–3515. [PubMed: 11929234]

6. Saab-Ismail NH, Simor T, Gaszner B, Lorand t, Szollosy M, Eglavish GA. Synthesis and in vivo evaluation of new contrast agents for cardiac MRI. J. Med. Chem 1999;42:2852–2861. [PubMed: 10425094]
7. Lu Z-R, Wang X, Parker DL, Goodrich KC, Buswell HR. Poly(l-glutamic acid) Gd(III)-DOTA conjugate with a degradable spacer for magnetic resonance imaging. Bioconjugate Chem 2003;14:715–719.
8. Achilefu S, Bloch S, Markiewicz MA, Zhong T, Ye Y, Dorshow RB, Chance B, Liang K. Synergistic effects of light-emitting probes and peptides for targeting and monitoring integrin expression. PNAS 2005;102:7976–7981. [PubMed: 15911748]
9. Miao Y, Whitener D, Feng W, Owen NK, Chen J, Quinn TP. Evaluation of the human melanoma targeting properties of radiolabeled α-melanocyte stimulating hormone peptide analogues. Bioconjugate Chem 2003;14:1177–1184.
10. Zhang Z, Liang K, Bloch S, Berezin M, Achilefu S. Monomolecular multimodal fluorescence-radioisotope imaging agents. Bioconjugate Chem 2005;16:1232–1239.
11. Lewis MR, Jia F, Gallazzi F, Wang Y, Zhang J, Shenoy N, Lever SZ, Hannink M. Radiometal-labeled peptide-PNA conjugates for targeting *bcl-2* expression: preparation, characterization, and in vitro mRNA binding. Bioconjugate Chem 2002;13:1176–1180.
12. Schottelius M, Schwaiger M, Wester H-J. Rapid and high-yield solution-phase synthesis of DOTA-Tyr^3-octoreotide and DOTA-Tyr^{3+}-octoreotate using unprotected DOTA. Tetrahedron Lett 2003;44:2393–3496.
13. De Leon-Rodriguez LM, Kovacs Z, Dieckmann GR, Sherry AD. Solid-phase synthesis of DOTA-peptides. Chem. Eur. J 2004;10:1149–1155.
14. Peterson JJ, Pak RH, Meares CF. Total solid-phase synthesis of 1,4,7,10- tetraazacyclododecane-N,N', N",N' "-tetraacetic acid-functionalized peptides for radioimmunotherapy. Bioconjugate Chem 1999;10:316–320.
15. Becker CF, Clayton D, Shapovalov G, Lester HA, Kochendoerfer GG. On-resin assembly of a linkerless lanthanide(III)-based luminescence label and its application to the total synthesis of site-specifically labeled mechanosensitive channels. Bioconjugate Chem 2004;15:1118–1124.
16. Albert R, Smith-Jones P, Stolz B, Simeon C, Knecht H, Bruns C, Pless J. Direct synthesis of [DOTA-$DPhe^1$]-octoreotide and [DOTA-$DPhe^1$,Tyr^3]-octoreotide (SMT487): two conjugates for systemic delivery of radiotherapeutical nuclides to somatostatin receptor positive tumors in man. Bioorg. Med. Chem. Lett 1998;8:1207–1210. [PubMed: 9871736]
17. Hsei H-P, Wu Y-T, Chen S-T, Wang K-T. Direct solid-phase synthesis of octoreotide conjugates: precursors for use as tumor-targeted radiopharmaceuticals. Bioorg. Med. Chem 1999;7:1797–1803. [PubMed: 10530927]
18. Gali H, Sieckman GL, Hoffman TJ, Owen NK, Mazuru DG, Forte LR, Volkert WA. Chemical synthesis of *Escherichia Coli* ST_h analogues by regioselective disulfide bond formation: biological evaluation of an ^{111}In-DOTA-Phe^{19}-ST_h analogue for specific targeting of human colon cancers. Bioconjugate Chem 2002;13:224–231.
19. Graham KA, Wang Q, Eisenhut M, Haberkorn U, Mier W. A general method for functionalizing both the C- and N-terminals of Tyr^3-octoreotate. Tetrahedron Lett 2002;43:5021–5024.
20. Lewis MR, Kao JY, Anderson AL, Shively JE, Raubitschek A. An improved method for conjugating monoclonal antibodies with N-hydroxysulfosuccinimidyl DOTA. Bioconjug Chem 2001;12:320–324. [PubMed: 11312695]
21. Chappell LL, Rogers BE, Khazaeli MB, Mayo MS, Buchsbaum DJ, Brechbiel MW. Improved synthesis of the bifunctional chelating agent 1,4,7,10-tetraaza-N-(1-carboxy-3-(4-nitrophenyl) propyl)-N',N",N"'-tri s(acetic acid)cyclododecane (PA-DOTA). Bioorg. Med. Chem 1999;7:2313–2320. [PubMed: 10632041]
22. Kruper WJ, Rudolf PR Jr. Langhoff CA. Unexpected selectivity in the alkylation of polyazamacrocycles. J. Org. Chem 1993;58:3869–3876.
23. Fields CG, Lloyd DH, Macdonald RL, Otteson KM, Noble RL. HBTU activation for automated Fmoc solid-phase peptide synthesis. Peptide Res 1991;4:95–101. [PubMed: 1815783]

24. Beck-Sickinger AG, Durr H, Jung G. Semiautomated T-bag peptide synthesis using 9-fluorenyl-methoxycarbonyl strategy and benzotriazol-1-yl-tetramethyl-uronium tetrafluoroborate activation. Peptide Res 1991;4:88–94. [PubMed: 1815782]
25. Kaiser E, Colescott RL, Bossinger CD, Cook PI. Color test for detection of free terminal amino groups in the solid-phase synthesis of peptides. Anal. Biochem 1970;34:595–598. [PubMed: 5443684]
26. Sarin VK, Kent SB, Tam JP, Merrifield RB. Quantitative monitoring of solid-phase peptide synthesis by the ninhydrin reaction. Anal. Biochem 1981;117:147–157. [PubMed: 7316187]
27. Madder A, Farcy N, Hosten NGC, Muynck HD, De Clercq PJ, Barry J, Davis AP. A novel sensitive colorimetric assay for visual detection of solid-phase bound amines. Eur. J. Org. Chem. 1999278722791
28. Pippin CG, Parker TA, McMurry TJ, Brechbiel MW. Spectrophotometric method for the determination of a bifunctional DTPA ligand in DTPA-monoclonal antibody conjugates. Bioconjugate Chem 1992;3:342–345.
29. Rohwer H, Collier N, Hosten E. Spectrophotometric study of arsenazo III and its interactions with lanthanides. Analytica Chimica Acta 1995;314:219–223.
30. Ward KM, Aletras AH, Balaban RS. A new class of contrast agents for MRI based on proton chemical exchange dependent saturation transfer (CEST). J. Magn. Reson 2000;143:79–87. [PubMed: 10698648]
31. Zhang S, Merritt M, Woessner DE, Lenkinski RE, Sherry AD. PARACEST agents: modulating MRI contrast via water proton exchange. Acc. Chem. Res 2003;36:783–790. [PubMed: 14567712]
32. Gopi HN, Suresh Babu VV. Zinc-promoted simple synthesis of oligomer-free N(α)-Fmoc-amino acids using Fmoc-Cl as an acylating agent under neutral conditions. J. Peptide Res 2000;55:295–299. [PubMed: 10798374]
33. Fields, GB.; Tian, Z.; Barany, G. Synthetic Peptides-A User's Guide. Grant, GA., editor. New York: W. H. Freeman; 1992. p. 77-183.
34. Tsujimoto T, Murai A. Efficient Detachment of N-Benzyl Carbamate Group. Synlett 2002;8:1283–1284.
35. Gisin BF. The monitoring of reactions in solid-phase peptide synthesis with picric acid. Anal. Chim. Acta 1972;58:248–249. [PubMed: 5057745]
36. King DS, Fields CG, Fields GB. A cleavage method which minimizes side reactions following Fmoc solid phase peptide synthesis. Int. J. Peptide Protein Res 1990;36:255–266. [PubMed: 2279849]
37. Albericio F, Kneib-Cordonier N, Biancalana S, Gera L, Masada RI, Hudson D, Barany G. Comparison of methods for the Fmoc solid-phase synthesis and cleavage of a peptide containing both tryptophan and arginine. J. Org. Chem 1990;55:3730–3743.
38. Riniker, B.; Hartmann, A. Peptides: Chemistry, Structure, and Biology. Rivier, JE.; Marshall, GR., editors. 1990. p. 950-952.
39. Fujisawa F, Mori T, Fukumoto K, Sato T. N,N,N',N'-Tetramethylchloroformamidinium chloride as an efficient condensation reagent for a novel esterification applicable to the macrolide synthesis. Chem. Lett 1982;11:1891–1894.
40. Dhaon MK, Olsen RK, Ramasamy K. Esterification of N-protected α-amino acids with alcohol/carbodiimide/4-(dimethylamino)pyridine. Racemization of aspartic and glutamic acid derivatives. J. Org. Chem 1982;47:1962–1965.
41. Bianchi A, Calabi L, Giorgi C, Losi P, Mariani P, Palano D, Paoli P, Rossi P, Valtancoli B. Thermodynamic and structural aspects of manganese(II) complexes with polyaminopolycarboxylic ligands based upon 1,4,7,10-tetraazocyclododecane (cyclen). Crystal structure of dimeric [MnL]$_2$2CH$_3$OH containing the new lignad 1,4,7,10-tetraaza-cyclododecane-1,4-diacetate. Dalton Trans 2001;2001:917–922.
42. Woods M, Aime S, Botta M, Howard JAK, Moloney JM, Navet M, Parker Db, Port M, Rousseaux O. Correlation of water exchange rate with isomeric composition in diastereomeric gadolinium complexes of tetra(carboxyethyl)dota and related macrocyclic ligands. J. Am. Chem. Soc 2000;122:9871–9792.
43. Dunand FA, Dickins RS, Parker D, Merbach AE. Towards rational design of fast water-exchanging Gd(dota-like) contrast agents? Importance of the M/m ratio. Chemistry--A European Journal 2001;7(23):5160–5167.

44. Zhang S, Kovacs Z, Burgess S, Aime S, Terreno E, Sherry AD. [DOTA-bis(amide)]lanthanide complexes: NMR evidence for differences in water-molecule exchange rates for coordination isomers. Chemistry, A European Journal 2001;7(1):288–296.
45. Williams RM, Aldous DJ, Aldous SC. General synthesis of β,γ-alkynylglycine derivatives. J. Org. Chem 1990;55:4657–4663.
46. Bodanszky, M.; Bodanszky, A. The practice of peptide synthesis. Berlin: Springer-Verlag; 1984. p. 153-158.
47. Sanchez IH, Lopez FJ, Soria JJ, Larraza MI, Flores HJ. Total synthesis of (±)-elwesine, (±)-epielwesine, and (±)-oxocrinine. J. Am. Chem. Soc 1983;105:7640–7643.
48. Winkler JD, Scott RD, Williard PG. Asymmetric induction in the vinylogous amide photocyclo addition reaction. A formal synthesis of vindorosine. J. Am. Chem. Soc 1990;112:8971–8975.
49. Subhas BD, Thurston DE. Boron trifluoride promoted cleavage of benzyl carbamates. Tetrahedron Lett 1990;31:6903–6906.
50. Bolos J, Perez-Beroy A, Gubert S, Anglada L, Sacristan A, Orbitz JA. Asymmetric synthesis of pyrrolo[2,1-b][1,3,4]thiadiazepine derivatives. Tetrahedron 1992;48:9567–9576.
51. Ihara M, Taniguchi N, Noguchi K, Fukumoto K, Kametani T. Total synthesis of hydrocinchonidine and hydrocinchonine via photooxygenation of an indole derivative. J. Chem. Soc. Perkin trans 1988;1:1277–1281.
52. Ferreira VF, Pinheiro S, Perrone CC, Costa PRR. Synthesis of new chiral auxiliares from carbohydrates for Et_2AlCl-promoted Diels-Alder reactions. J. Braz. Chem. Soc 2000;11:266–273.
53. Yang D, Gao Q, Zheng BF, Zhu NY. Et2AlCl-promoted asymmetric phenylseleno group transfer radical cyclization reactions of unsaturated β-hydroxy esters. J. Org. Chem 2004;69:8821–8828. [PubMed: 15575763]
54. Li G, Wei HX, Whiteney BR, Batrice NN. Novel asymmetric C-C bond formation process promoted by Et2AlCl and its application to the stereoselective synthesis of unusual β-branched Baylis0Hillman adducts. J. Org. Chem 1999;64:1061–1064. [PubMed: 11674192]
55. Garcia-Calvo M, Peterson EP, Leiting B, Ruel R, Nicholson DW, Thornberry NA. Inhibition of human caspases by peptide-based and macromolecular inhibitors. J. Biol. Chem 1998;273:32608–32613. [PubMed: 9829999]
56. Paul-Roth C, Raymond KN. Amide Functional Group Contribution to the Stability of Gadolinium (III) Complexes: DTPA Derivatives. Inorg. Chem 1995;34:1408–1412.
57. Sarka L, Burai L, Kiraly R, Zekany L, Brucher E. Studies on the kinetic stabilities of the Gd (3+) complexes formed with the N-mono(methylamide), N'-mono(methylamide) and N,N"- bis (methylamide) derivatives of diethylenetriamine-N,N,N',N",N"-pentaacetic acid. J. Inorg. Biochem 2002;91:320–326. [PubMed: 12121791]
58. Aime S, Barge A, Castelli DD, Fedeli F, Mortillaro A, Nielson FU, Terreno E. Paramagnetic lanthanide(III) complexes as pH-sensitive chemical exchange saturation transfer (CEST) contrast agents for MRI applications. Magn. Reson. Med 2002;47:639–648. [PubMed: 11948724]
59. Peters, JA.; Zitha-Bovens, E.; Corsi, DM.; Geraldes, CFGC. The chemistry of contrast agents in medicinal magnetic resonance imaging. Merbach, AE.; Toth, E., editors. New York: Wiley; 2001. Ch. 8
60. Kodama M, Koike T, Mahatma AB, Kimura E. Thermodynamic and kinetic studies of lanthanide complexes of 1,4,7,10,13-pentaazacyclopentadecane-N,N',N",N"',N"' #x00027;-pentaacetic acid and 1,4,7,10,13,16-hexaazacyclooctadecane-N,N',N"',N"',N' "',N""'-hexaacetic acid. Inorganic Chemistry 1991;30:1270–1273.
61. Chu SC, Pike MM, Fossel ET, Smith TW, Balschi JA, Springer SS. Aqueous shift reagents for high resolution cationic nuclear magnetic resonance III $Dy(TTHA)^{3-}$, $Tm(TTHA)^{3-}$ and $Tm(PPP)_2^{7-}$. J. Magn. Reson 1984;56:33–47.
62. Elst LV, Roch A, Gillis P, Laurent S, Botteman F, Bulte JWM, Muller R. Dy-DTPA derivatives as relaxation agents for very high field MRI: The beneficial effect of slow water exchange on the transverse relaxivities. Magon Resn. Med 2000;47:1121–1130.
63. Chen X, Liu S, Hou Y, Tohme M, Park R, Bading JR, Conti PS. MicroPET imaging of breast cancer αv-Integrin expression with 64Cu-labeled dimeric RGD peptides. Molecular Imaging and Biology 2004;6:350–359. [PubMed: 15380745]

64. Rodrigues M, Traub-Weidinger T, Li S, Ibi B, Virgolini I. Comparison of 111In-DOTA-Dphe1-Tyr3-octreotide and 111In-DOTA-lanreotide scintigraphy and dosimetry in patients with neuroendocrine tumours. Eur. J. Nucl. Med. Mol. Imaging 2006;33:532–540. [PubMed: 16491425]

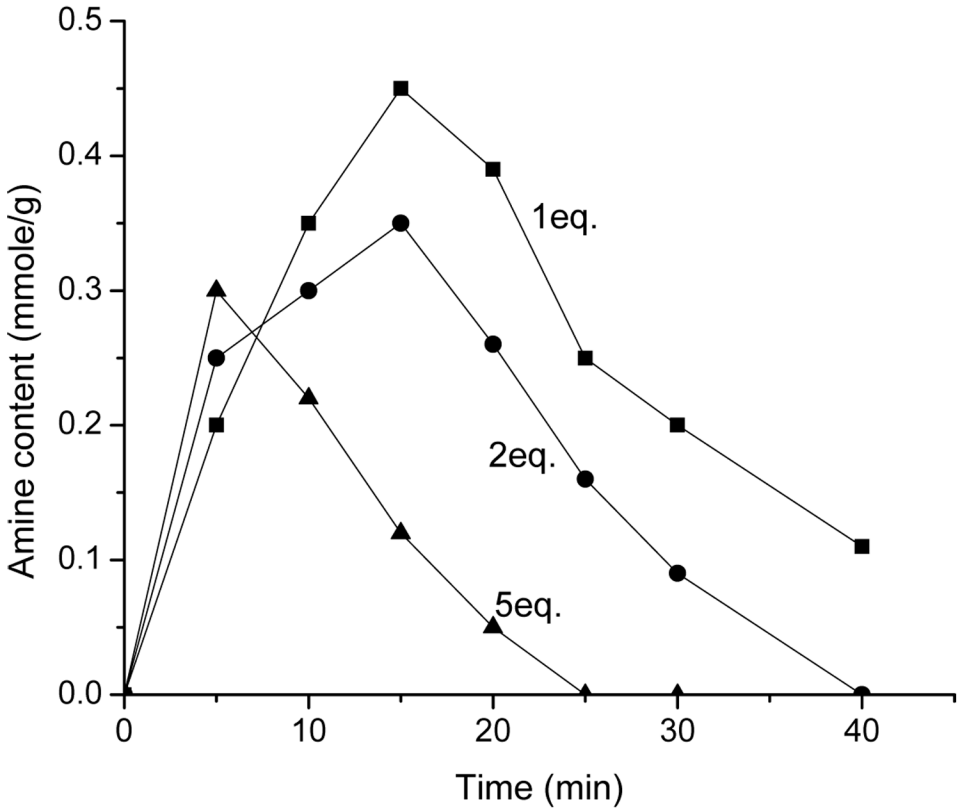

Figure 1.

The amine content following CBZ cleavage versus reaction time. For 5eq. of Et_2AlCl/thioanisole, the reaction was too fast to control the cleavage of CBZ group and benzyl ether linker group. 1eq. of Et_2AlCl/thioanisole showed the best CBZ cleavage conditions and a similar reaction rate was obtained with 2eq. of Et_2AlCl. The optimized CBZ cleavage reaction was carried out for 15 min with 1eq. of Et_2AlCl at −78°C.

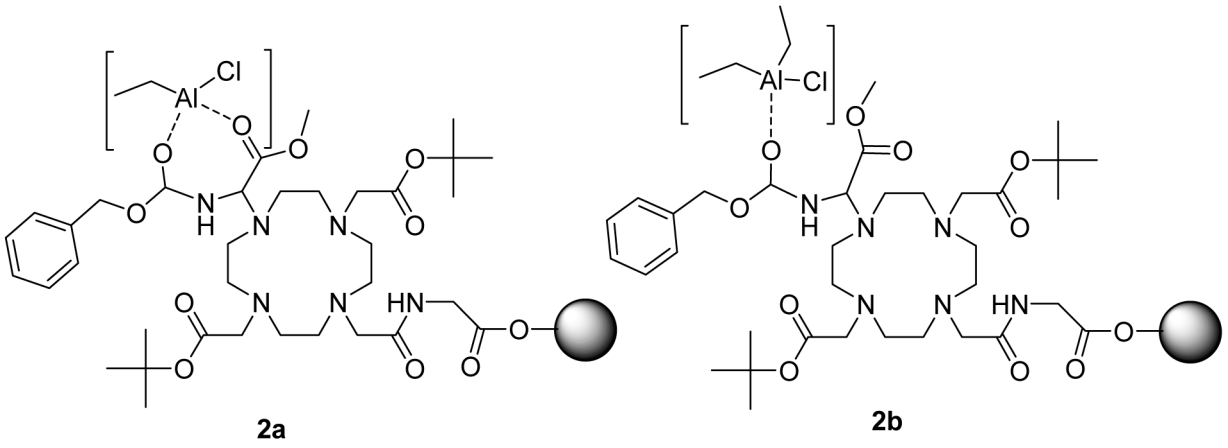

Figure 2.

Two possible transition states of Et_2AlCl and CBZ-aminoDOTA Wang resin. The transition state in Figure 2a shows the bridging of Et_2AlCl between two carbonyl groups. This arrangement requires the formation of an unstable 7-membered ring that also suffers from planar constraints of the amide and ester groups. Figure 2b represents a more stable interaction that forms a single bond between Et_2AlCl and one carbonyl group. This single-bond transition state is supported by mass spectral results of **10a** and **10b**.

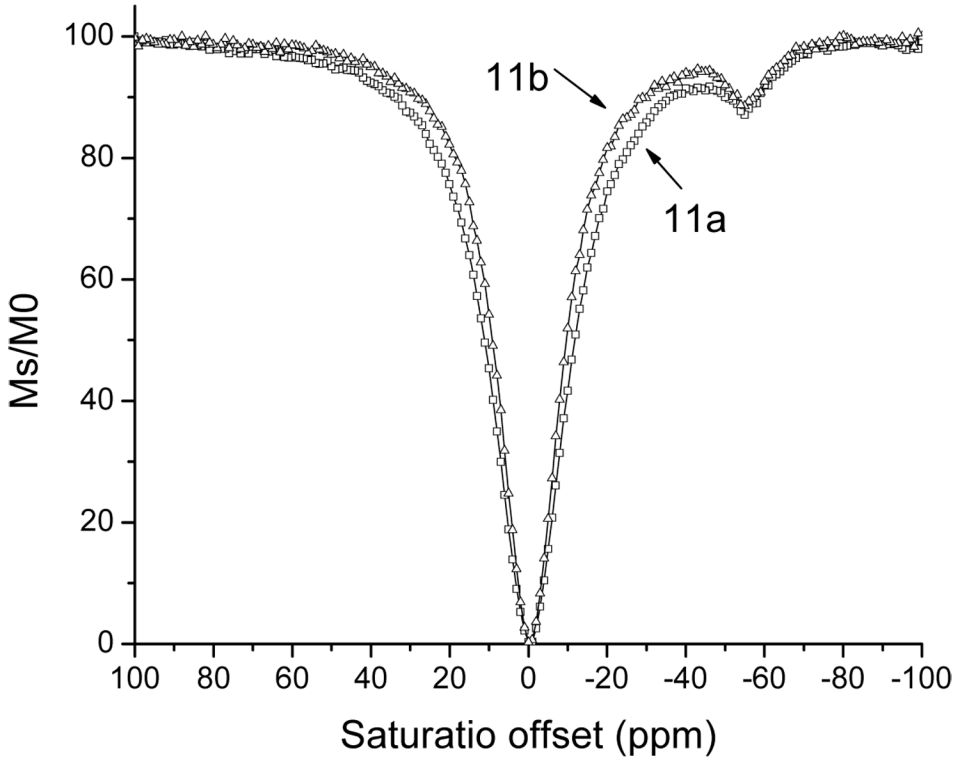

Figure 3.

The PARACEST spectrum of **11a** (25mM in 5% D2O in H2O) and **11b** (12mM in 5% D2O in H2O). PARACEST spectra were acquired using a Varian Inova 600 MHz NMR spectrometer with a modified presaturation pulse sequence that included a continuous wave saturation pulse, saturation pulse power of 31μT, saturation delay of 4 seconds. The 1D NMR spectra of water used to construct the PARACEST spectra were acquired with saturation in 1 ppm increments from 100 ppm to −100 ppm.

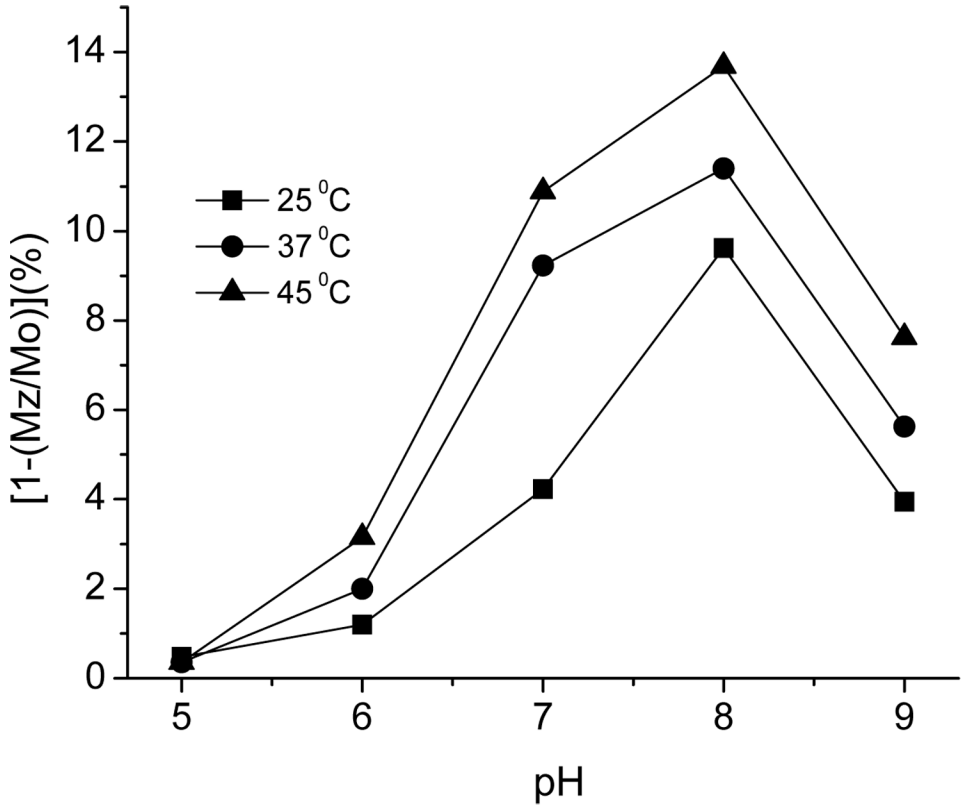

Figure 4.

The effect of pH and temperature on the PARACEST effect of 25 mM of **11a**. PARACEST spectra were acquired using a Varian Inova 600 MHz NMR spectrometer with a modified presaturation pulse sequence that included a continuous wave saturation pulse, saturation pulse power of 31μT, saturation delay of 4 seconds at −51ppm and +51ppm.

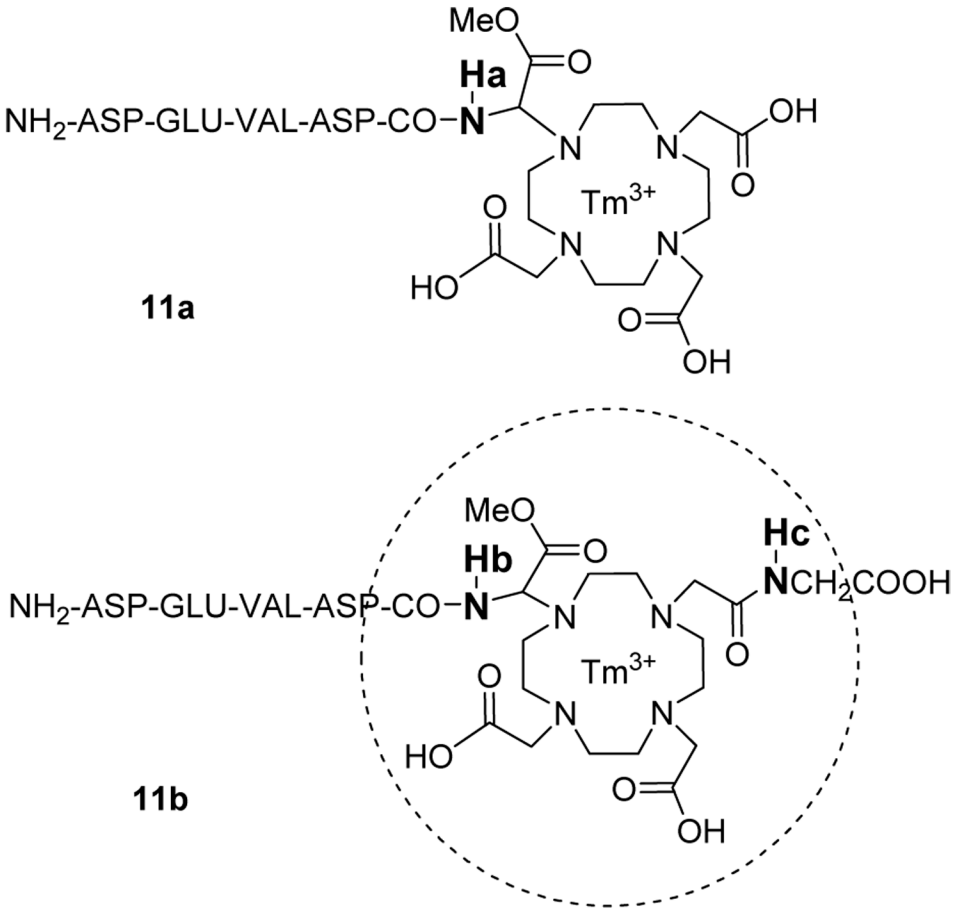

Figure 5.

The proximity of amide hydrogens to Tm^{3+} in **11a** and **11b**. Molecular modeling results indicated that Hb is positioned 4.1–4.3 angstroms from Tm^{3+}, and Hc is positioned 4.9–5.1 angstroms from Tm^{3+}. The dotted line of the 2D schematic is 5.4 angstroms from the lanthanide ion, and is provided as a visual aid. The PARACEST effects from two different amide hydrogens Hb and Hc were not distinguishable, as only one PARACEST effect was detected at −51ppm, which is consistent with the similar proximities of these hydrogens to the Tm^{3+}.

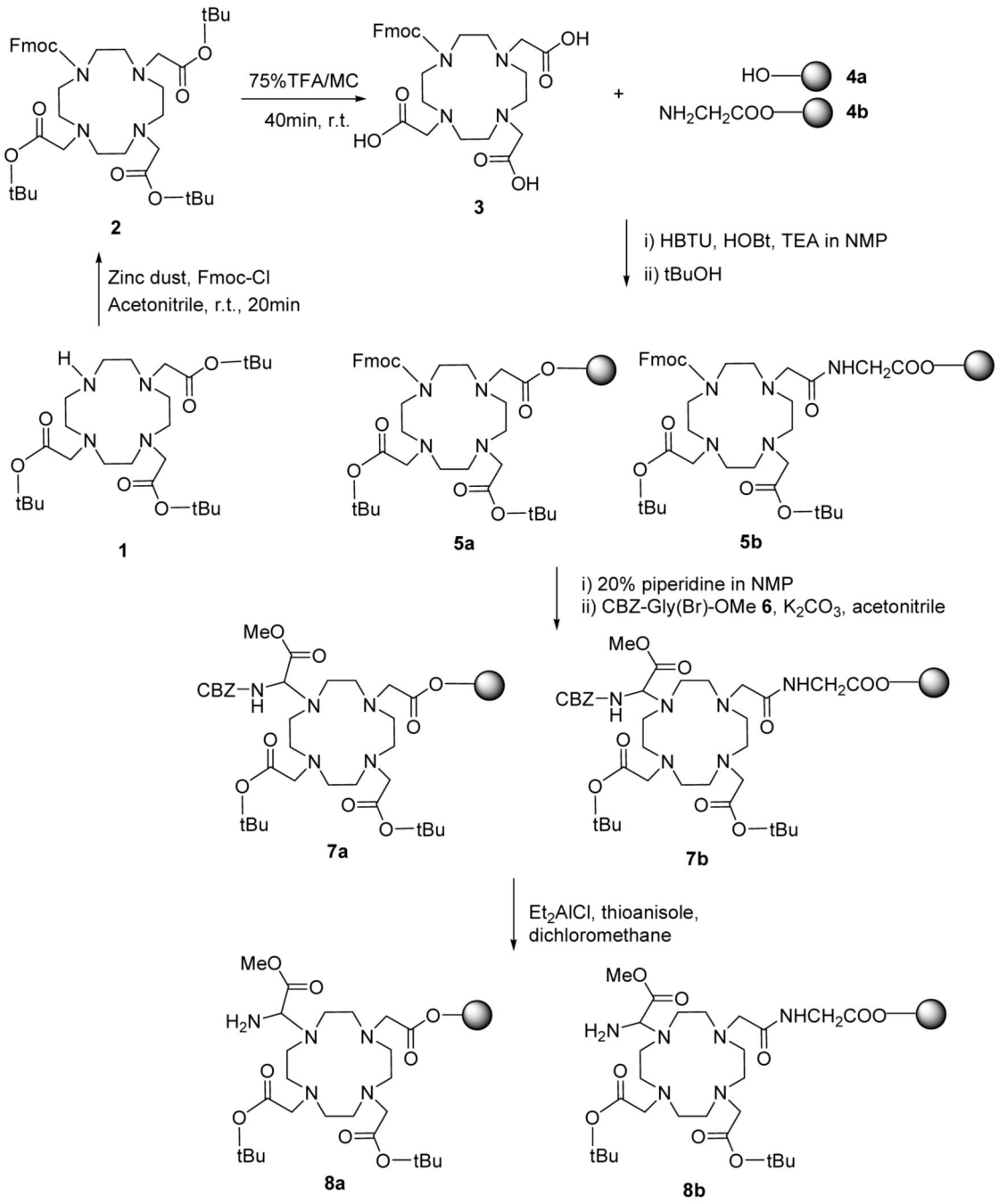

Scheme 1. Preparation of amino-DOTA pre-loaded polymeric support

For clarity, **5a–8a** and **5b–8b** only show ligands coupled to the cyclen ring in a 1,4 configuration. However, a 1,7 configuration is also possible.

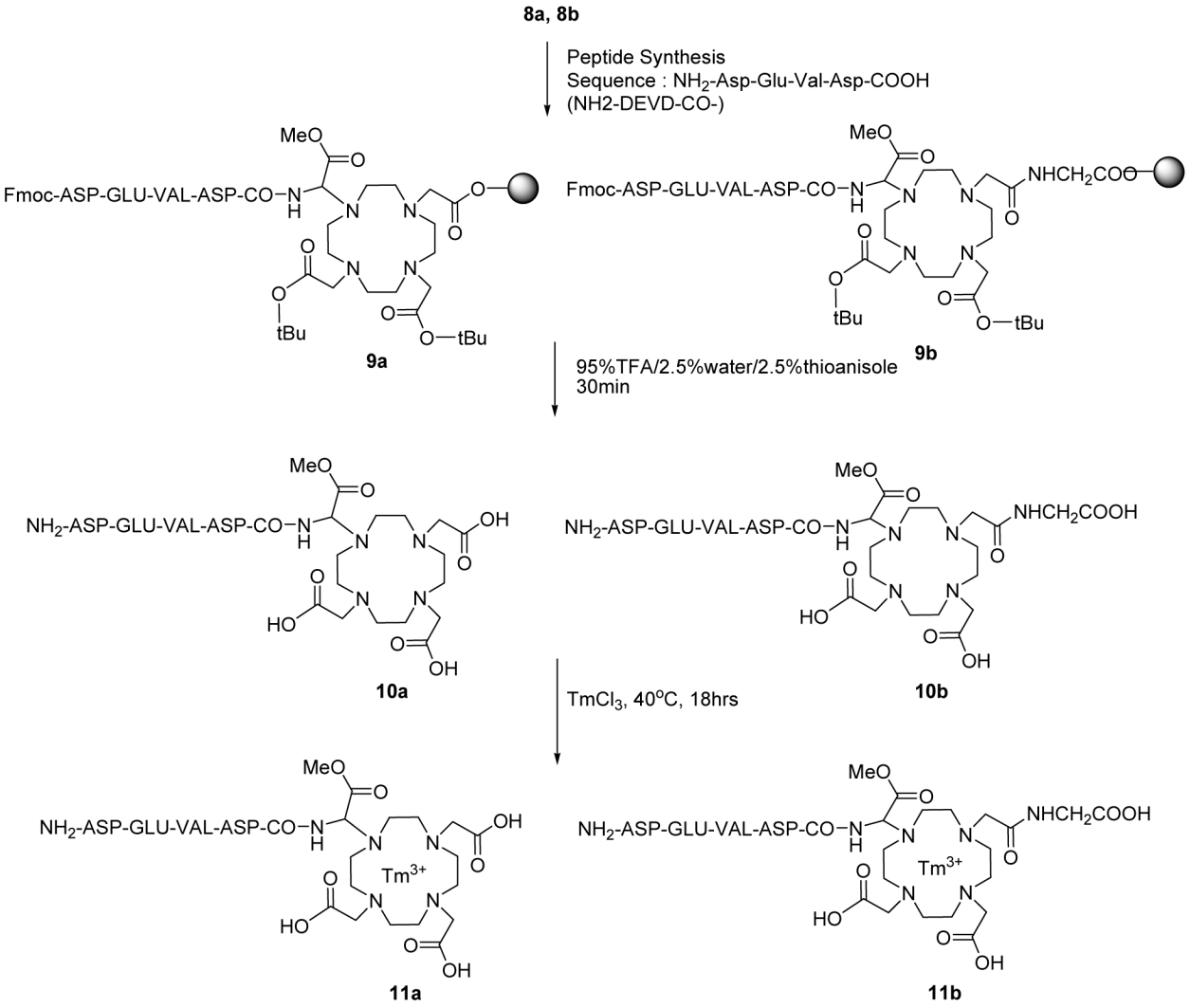

Scheme 2. Synthesis of peptidyl contrast agents

For clarity, **8a–9a** and **8b–11b** only show ligands coupled to the cyclen ring in a 1,4 configuration. However, a 1,7 configuration is also possible.